Integration and Validation of 3GPP TR 38.811 Aligned GEO NTN-TDL Channel Models in OpenAirInterface5G

Sumit Kumar*, Ion Turcanu*, Sebastien Faye*
*Luxembourg Institute of Science and Technology
{sumit.kumar, ion.turcanu, sebastien.faye}@list.lu

Accepted for presentation at the 2026 IEEE Future Networks World Forum (FNWF), Main Track T02: Non-terrestrial networks (NTN) – satellite/HAPS/UAV and their integration with terrestrial networks; satellite networks.

***Abstract*—This paper presents the integration of 3GPP TR 38.811-based NTN tapped-delay-line (TDL) channel models into the OpenAirInterface5G (OAI) RF simulator (RFsim) for controlled end-to-end geostationary (GEO) non-terrestrial network (NTN) experimentation. Currently OAI RFsim channel models do not include standardized NTN-specific multipath profiles and elevation-dependent large-scale channel effects. Such effects are important for evaluating frequency selectivity, received signal strength, and their impact on PHY and end-to-end system performance. Our implementation incorporates the NTN-TDL-A/B/C/D profiles, elevation-dependent large-scale attenuation, explicit line-of-sight (LOS) and non-line-of-sight (NLOS) state handling, and initialization-time profile-selection policy. Validation is performed at three levels combining channel-model descriptor checks, PHY-level BLER evaluation, and end-to-end 5G SA trials across multiple channel profiles, elevation angles, and LOS/NLOS conditions. The results confirm the expected channel behavior, profile selection, and successful user-plane establishment. The implementation enables reproducible end-to-end 5G-NTN experiments in OAI under representative TR 38.811-based GEO channel conditions.**

I. Introduction

Fifth-generation Non-Terrestrial Networks (5G-NTN) extend cellular connectivity through satellites in geostationary (GSO) and non-geostationary (NGSO) orbits. 3GPP TR 38.811 [1] defines representative NTN channel models, including tapped-delay-line (TDL) small-scale fading profiles A/B/C/D and large-scale effects such as elevation-dependent free-space path loss, clutter loss, shadow fading, and LOS/NLOS conditions. Incorporating these channel effects into a complete 5G protocol stack is important because NTN multipath and large scale attenuation determine frequency selectivity and received signal strength. These effects influence synchronization, channel estimation, equalization, link adaptation, retransmissions, and end-to-end performance.

OpenAirInterface5G (OAI) [2], an open-source implementation of the 5G protocol stack, provides a suitable platform for end-to-end NTN experimentation. Its RF simulator (RFsim) supports fixed for GEO scenarios, however, the baseline GEO configuration does not combine these effects with the standardized NTN-TDL multipath profiles and elevation-dependent large-scale terms as defined in TR 38.811. Consequently, OAI RFsim cannot represent their combined impact in full-stack GEO experiments, motivating their integration into OAI RFsim.

This work integrates TR 38.811-based GEO NTN channel models into OAI RFsim. The implementation combines the standardized TDL-A/B/C/D small-scale fading profiles with elevation-dependent large-scale attenuation and configurable LOS/NLOS state handling. It also introduces an OAI-specific profile-selection policy that consistently associates the effective TDL profile with the resolved link state.

The main contributions are as follows:

1) Integration of the TR 38.811 TDL-A/B/C/D small-scale fading profiles (Sec. 6.9.2) into OAI RFsim.
2) Integration of elevation-dependent path loss, clutter loss, and NLOS shadow fading based on TR 38.811 Sec. 6.6.2. Link reciprocity is maintained by applying the same large-scale NLOS shadow-fading offset to the downlink and uplink RFsim paths.
3) Configurable LOS/NLOS state handling, including deterministic random-state selection based on the elevation-dependent TR 38.811 LOS probability.
4) Definition and implementation of four OAI-specific composite channel models, `SAT_GEO_NTN_TDL_A/B/C/D`, including an initialization-time profile-selection policy consistent with the TR 38.811 association of profiles A/B with NLOS and C/D with LOS conditions.
5) Validation through channel-model checks, PHY-level BLER evaluation, and sixteen end-to-end RFsim trials covering all four configured TDL types, two elevation angles, and both LOS and NLOS states.

All end-to-end trials within RFsin environment selected the expected effective profiles and successfully completed UE registration and user-plane establishment.

The remainder of this paper is organized as follows. Section II reviews related work, Section III describes the baseline OAI channel model and its gaps, Section IV presents the proposed implementation, Section V reports the validation results, and Section VI concludes the paper.

II. Related Work

At the link level, the MathWorks `nrTDLChannel` implements the TR 38.811 NTN-TDL-A/B/C/D profiles and supports waveform- and link-level evaluation, but it does not provide an end-to-end 5G protocol stack [3]. OpenNTN extends Sionna with TR 38.811 based scenario, large-scale, and cluster ray channel modelling; however, its current implementation does not include the NTN-TDL-A/B/C/D profiles of Sec. 6.9.2 [4].

At higher abstraction and full-stack levels, Sandri *et al.* integrate TR 38.811 mobility, large-scale propagation effects, scintillation, and the Sec. 6.7.2 cluster–ray model into ns-3, where multipath is generated through clusters and constituent rays with statistical delays, powers, and angles [5]. Similarly, SNS3 supports constellation, scheduling, routing, and packet-level satellite-network studies, but is not intended for sample-level NR PHY validation over NTN-TDL channels [6].

At the full-stack level, OCUDU (formerly srsRAN) demonstrates Release-17 NTN timing and end-to-end connectivity using a delay-only GNU Radio/ZeroMQ GEO channel emulator; however, multipath fading and large-scale propagation effects are not included [7], [8].

Prior OAI studies demonstrated NTN timing, synchronization, and end-to-end connectivity over emulated and live satellite links [9]–[13]; however, they did not integrate the TR 38.811 NTN-TDL profiles with elevation-dependent large-scale propagation and configurable LOS/NLOS states within RFsim.

Overall, existing platforms address complementary aspects of NTN evaluation, ranging from link-level fading and cluster–ray modelling to packet-level satellite-network simulation and full-stack connectivity. However, none of the reviewed full-stack platforms combines the TR 38.811 NTN-TDL-A/B/C/D profiles with elevation-dependent large-scale attenuation and configurable LOS/NLOS states.

Our work fills this gap by integrating these channel components directly within OAI RFsim [2].

III. OAI RFsim Baseline and Extensions

A. Baseline Channel Model and Gap

Before this work, OAI GEO RFsim experiments used a single-path link with configured propagation delay and SIB19 timing assistance. Although terrestrial `TDL_A/B/C/D/E` models were available, RFsim lacked a composite GEO channel model combining the TR 38.811 Sec. 6.9.2 NTN-TDL profiles with the elevation-dependent large-scale terms of TR 38.811 Sec. 6.6. In particular, it did not provide:

- The `NTN_TDL_A/B/C/D` small-scale fading profiles;
- Elevation-dependent relative free-space path loss and clutter loss;
- Scenario- and elevation-dependent NLOS shadow fading; or
- Configurable LOS/NLOS state handling based on Table 6.6.1-1 P_{LOS} from TR 38.811.

The absence of these effects limits controlled evaluation of frequency-selective propagation and received-power variation within the complete OAI protocol stack.

Building on OAI's existing GEO delay, Doppler, and SIB19 timing support, we introduced the channel-model extensions summarized in Table I. Section IV-A describes how these channel components are implemented in OAI RFsim.

IV. Implementation in OAI

The new GEO composite channel models extend the existing RFsim satellite link processing with TR 38.811 based small and large scale channel effects. RFsim continues to apply the bulk GEO propagation delay, while the channel-model path introduces excess multipath and elevation and state dependent attenuation. A common LOS/NLOS state maintains consistency between the selected fading profile and the associated large-scale terms. The following subsections distinguish the TR 38.811-derived components from the OAI-specific implementation choices.

A. NTN-TDL Small-Scale Profiles

a) TR 38.811 NTN-TDL Profile Definition.: An NTN-TDL profile represents multipath propagation as a set of discrete delayed signal components, called taps. For each tap, Sec. 6.9.2 in TR 38.811 specifies a normalized excess delay and a relative average power. The actual delay of tap l is obtained from

$$\tau_l = \tilde{\tau}_l DS, \tag{1}$$

where $\tilde{\tau}_l$ is the normalized delay and DS is the configured RMS delay spread. The profile therefore defines the relative tap structure, whereas DS controls the absolute tap spacing and resulting frequency selectivity.

Furthermore, channel profiles A and B represent NLOS propagation and contain Rayleigh-faded taps. While profiles C and D represent LOS propagation; their first taps are Ricean with $K_1 = 10.224$ dB and $K_1 = 11.707$ dB, respectively, while their remaining taps are Rayleigh faded. These profiles are specified at a 50° reference elevation and are summarized in Table II.

b) Implementation in OAI.: OAI implements the four profiles as `NTN_TDL_A/B/C/D` descriptors in the existing RFsim `chanmod` TDL processing path (`random_channel.c`). During initialization, OAI loads the TR 38.811 relative tap powers and Ricean K-factors and multiplies the normalized delays by the configured `ds_tdl` value. The resulting discrete-time FIR is formed as

$$g[k] = \sum_{\ell=0}^{L-1} a_\ell \,\mathrm{sinc}(k - f_s\tau_\ell)\,, \qquad \tau_\ell = \tilde{\tau}_\ell d_s \tag{2}$$

with

$$\mathrm{E}\big[|a_\ell|^2\big] = p_\ell, \qquad \sum_{\ell=0}^{L-1} p_\ell = 1, \tag{3}$$

where $g[k]$ is the discrete-time FIR response at sample index k, L is the number of taps, ℓ is the tap index, a_ℓ is the complex

TABLE I
BASELINE OAI GEO RFSIM CAPABILITIES AND EXTENSIONS INTRODUCED IN THIS WORK

Component	Baseline OAI GEO RFsim	Extension introduced in this work	Utility
Satellite dynamics	Bulk propagation delay and Doppler support	Retained and combined with the new GEO channel components	Preserve GEO timing and satellite-motion effects
Small-scale fading	No NTN-specific TDL profiles in the GEO configuration; terrestrial TDL models were available separately	TR 38.811 NTN-TDL-A/B/C/D tap profiles	Represent NTN-specific frequency-selective multipath fading
Large-scale attenuation	No elevation- and state-dependent GEO correction	Relative FSPL and clutter corrections referenced to 90°, with NLOS shadow fading	Represent elevation- and state-dependent received-power variation
Link state	No explicit GEO LOS/NLOS resolver	Configurable `los`, `nlos`, and `random` states	Enable controlled and repeatable LOS/NLOS conditions
Profile selection	No state-dependent NTN-TDL selection	Initialization-time selection between the OAI-specific A/C and B/D profile pairs	Associate the effective tap configuration with the resolved state
Composite channel	GEO delay and NTN multipath/large-scale effects not combined	Four `SAT_GEO_NTN_TDL_A/B/C/D` channel types	Configure timing, multipath, and large-scale effects as one GEO channel

TABLE II
NTN-TDL SMALL-SCALE PROFILES FROM TR 38.811 SEC. 6.9.2 (50° REFERENCE; DELAYS SCALED AT RUNTIME) [1]

Profile	Tbl.	Taps	State	Fading
`NTN_TDL_A`	6.9.2-1	3	NLOS	All Rayleigh
`NTN_TDL_B`	6.9.2-2	4	NLOS	All Rayleigh
`NTN_TDL_C`	6.9.2-3	2	LOS	Ricean, K_1=10.2 dB
`NTN_TDL_D`	6.9.2-4	3	LOS	Ricean, K_1=11.7 dB

coefficient of tap ℓ, p_ℓ is its normalized average power, $\tilde{\tau}_\ell$ is the normalized TR 38.811 delay, $d_s = \texttt{ds\_tdl}$, f_s is the sampling rate, and $\mathrm{sinc}(x) = \sin(\pi x)/(\pi x)$.

The bulk GEO propagation delay remains configured separately through `rfsimulator.prop_delay`. Consequently, the NTN-TDL taps represent only the excess multipath delays relative to the main signal arrival, rather than the satellite propagation time itself. For profiles C and D, the direct and scattered components occurring at the same first-tap delay are represented by one Ricean tap. The resulting frequency selectivity depends on both the selected profile and `ds_tdl`, as evaluated in Table V.

Accordingly, `channelmod.offset` is set to zero, while the bulk GEO delay remains on `rfsimulator.prop_delay` and is aligned with the SIB19 timing configuration. Channel modelling is enabled through `chanmod` in the paired gNB and UE RFsim configurations.

B. Elevation-Dependent Large-Scale Loss

a) TR 38.811 Large-Scale Parameter Definition.: TR 38.811 expresses the basic path loss as

$$PL_b = \mathrm{FSPL}(d, f_c) + SF + CL(\alpha, f_c), \tag{4}$$

where d is the satellite-to-terminal slant range, f_c is the carrier frequency, and α is the elevation angle. The slant range increases as the elevation decreases, resulting in greater free-space path loss.

Clutter loss CL represents attenuation caused by buildings and other objects around the ground terminal. It depends on the deployment environment, frequency band, and elevation angle. Under LOS conditions, TR 38.811 sets the clutter loss to zero. Under NLOS conditions, its value is selected from Tables 6.6.2-1–6.6.2-3 for dense-urban, urban, and suburban/rural environments, respectively.

Shadow fading SF is a zero-mean Gaussian random variable in decibels. TR 38.811 provides state-, scenario-, and elevation-dependent values of σ_{SF} for both LOS and NLOS conditions. Because the tabulated clutter and shadow-fading parameters are provided at 10° elevation intervals, TR 38.811 specifies using the reference angle nearest to the actual elevation. For example, 33° is mapped to 30°.

b) Implementation in OAI.: The implementation treats the configured RFsim path loss as the baseline at the 90° GEO reference. This 90° baseline is an OAI large-scale implementation reference and is distinct from the 50° reference elevation used in TR 38.811 Sec. 6.9.2 for the small-scale NTN-TDL profiles. To avoid applying the absolute GEO path loss twice, the implementation adds only the elevation-dependent FSPL correction

$$\Delta\mathrm{FSPL}(\alpha) = \mathrm{FSPL}(\alpha) - \mathrm{FSPL}(90^\circ). \tag{5}$$

For NLOS links, clutter is applied similarly as

$$\Delta CL(\alpha) = CL(\alpha) - CL(90^\circ), \tag{6}$$

whereas clutter is set to zero under LOS conditions. The clutter and shadow-fading parameters are selected from the TR 38.811 tables using the reference elevation nearest to the configured value.

The parameter `geo_elevation_deg` defaults to 90°; therefore, the FSPL and clutter corrections are zero unless a lower elevation is configured.

In the current implementation, shadow fading is enabled only for NLOS states. A zero-mean Gaussian offset is generated using the corresponding TR 38.811 NLOS standard deviation, and the same realization is applied to the gNB and UE RFsim paths to maintain link reciprocity. For LOS states, the shadow-fading standard deviation is set to zero. Runtime `GEO state` logs report the elevation, slant range,

TABLE III
OAI STATE-DEPENDENT PROFILE-SELECTION POLICY FOR GEO COMPOSITES

Configured composite	NLOS profile	LOS profile
SAT_GEO_NTN_TDL_A	A	C
SAT_GEO_NTN_TDL_B	B	D
SAT_GEO_NTN_TDL_C	A	C
SAT_GEO_NTN_TDL_D	B	D

FSPL correction, clutter correction, shadow-fading standard deviation and realization, and the total applied large-scale correction.

C. LOS/NLOS State Resolution and Profile Selection

a) TR 38.811 LOS-Probability and State Basis.: Table 6.6.1-1 specifies the LOS probability P_{LOS} as a function of elevation angle and deployment environment. TR 38.811 also associates NTN-TDL-A/B with NLOS propagation and NTN-TDL-C/D with LOS propagation. However, it does not define named GEO composite models, forced link states, or a policy for remapping between the profiles.

b) OAI policy and implementation.: OAI controls the GEO LOS/NLOS state through `geo_channel_state`, which accepts `los`, `nlos`, or `random`. The first two settings force the corresponding state for controlled testing. In `random` mode, OAI obtains P_{LOS} from Table 6.6.1-1 using the configured environment and nearest reference elevation. The link state is drawn once during initialization using a deterministic seed shared by the gNB and UE, ensuring that both sides resolve the same state.

The resolved state controls both the large-scale channel terms and the effective small-scale fading profile. To maintain consistency between them, the implementation defines two OAI-specific profile pairs: A/C and B/D. These pairings are implementation conventions and are not specified by TR 38.811. For the A/C pair, NLOS selects profile A and LOS selects profile C; for the B/D pair, NLOS selects profile B and LOS selects profile D. Table III shows the resulting mapping for all four configured composite channel types.

During initialization, `load_channellist()` uses the configured composite and resolved state to select the effective NTN-TDL profile before the taps are instantiated. A remapping log is emitted when the effective profile differs from the profile named in the configured composite.

V. Validation Methodology and Results

Validation is performed at three levels. First, channel-model checks verify the NTN-TDL descriptors, realized multipath structure, elevation-dependent parameters, and statistical LOS/NLOS behavior. Second, PHY-level tests evaluate the implemented profiles through downlink and uplink BLER measurements. Third, end-to-end RFsim trials verify consistent channel configuration across the gNB and UE and successful 5G SA connectivity. Table IV summarizes the common validation and simulation parameters used throughout this section.

TABLE IV
VALIDATION AND SIMULATION PARAMETERS USED IN SECTION V.

Parameter	Value
TDL delay-spread setting d_s	100 ns
Sampling rate f_s	7.68 MHz
NR bandwidth / PRBs	5 MHz / 25 PRBs
Numerology	$\mu = 0$ (15 kHz SCS)
Descriptor validation	NTN_TDL_A/B/C/D
Impulse-PDP averaging	50000 realizations/profile
Frequency-selectivity averaging	1000 realizations/profile
GEO statistical validation	50000 realizations
PHY point check	2 dB SNR
PHY BLER sweep	2–10.2 dB, 0.2 dB step, 2500 trials/point
End-to-end matrix	Urban; 30°, 60°; forced `los`/`nlos`; GEO composites A/B/C/D

TABLE V
OCCUPIED-BAND FREQUENCY SELECTIVITY OF THE IMPLEMENTED OAI FIR (7.68 MHZ SAMPLING, 4.5 MHZ OCCUPIED BANDWIDTH, 1000 REALIZATIONS PER CASE). EACH ENTRY REPORTS $|\rho|$ AND MEDIAN RMS MAGNITUDE RIPPLE.

Prof.	$d_s = 100$ **ns** $\lvert\rho\rvert$ / ripple	**30° urban mean** $\lvert\rho\rvert$ / ripple	**60° urban mean** $\lvert\rho\rvert$ / ripple
A (NLOS)	0.239 / 3.20 dB	0.822 / 0.88 dB	1.000 / 0 dB (1-tap)
B (NLOS)	0.329 / 1.94 dB	0.797 / 0.67 dB	0.930 / 0.49 dB (mild)
C (LOS)	0.991 / 0.36 dB	0.992 / 0.25 dB	0.996 / 0.17 dB
D (LOS)	0.889 / 1.00 dB	1.000 / 0 dB (1-tap)	1.000 / 0 dB (1-tap)

A. Channel-Model Validation

A standalone test constructed each `NTN_TDL_A/B/C/D` profile through the runtime OAI channel-creation path and verified its tap count, normalized delays and powers, channel-length estimate, and Ricean K-factors against TR 38.811. All checks matched the reference profiles summarized in Table II.

To verify the realized discrete-time channel, an impulse-input test averaged the power-delay profile over 50,000 realizations. At 7.68 MHz, taps separated by less than one sample cannot be resolved individually; therefore, the comparison is performed over resolved power clusters, grouping paths separated by less than one sample. Measured powers are normalized and assigned to the nearest cluster, and the cluster-L_1 error is defined as $L_1 = \sum_c |\hat{p}_c - p_c|$, where p_c and $\hat{p}_c$ are the expected and measured normalized cluster powers. The resulting cluster-L1 errors are 0.000912, 0.037666, 0.000206, and 0.006273 for profiles A/B/C/D, respectively, indicating close agreement with the intended power distributions.

The GEO resolver, which determines the LOS/NLOS state and associated elevation-dependent channel parameters, was tested over 50,000 realizations. Table VI shows that the LOS probabilities and NLOS shadow-fading spreads closely match TR 38.811, while the delay spreads and relative FSPL corrections follow the expected elevation trends.

In Table V, $|\rho|$ denotes the correlation magnitude between the channel responses at -2.25 and $+2.25$ MHz across the realizations. RMS ripple is the median per-realization RMS magnitude variation in dB after removing the mean over the 300 occupied subcarriers.

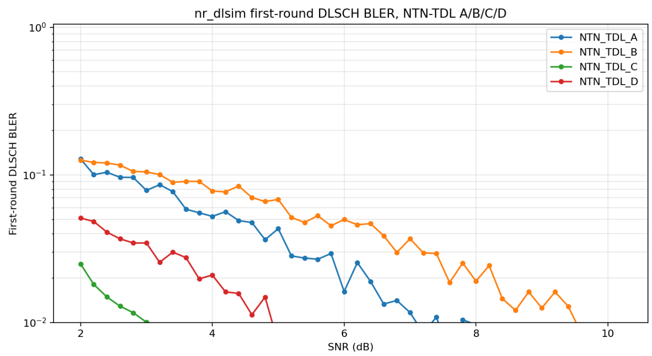

Fig. 1. `nr_dlsim` first-round DLSCH BLER vs. SNR for `NTN_TDL_A/B/C/D` (2500 trials/point, 0.2 dB steps).

At $d_s = 100$ ns, profiles A and B are strongly frequency-selective, profile D is moderately selective, and profile C is nearly flat. The smaller elevation-dependent delay spreads reduce this selectivity; at 60°, profiles A and D resolve to a single FIR tap at 7.68 MHz.

B. PHY-Level Validation

PHY-level tests used OAI's `nr_dlsim` and `nr_ulsim`, which are link-level simulators for the NR downlink and uplink, respectively. At 2 dB SNR, both simulators produced the BLER ordering `B > A > D > C`, as summarized in Table VII. This is used as a consistency check between the downlink and uplink implementations, not as a 3GPP conformance criterion.

Figure 1 extends the downlink evaluation from 2 dB to 10.2 dB in 0.2 dB steps, using 2500 trials per point. Under the evaluated configuration, profiles A and B exhibit higher BLER than profiles C and D, and the LOS-oriented profiles cross the 10^{-2} BLER level at lower SNR. The curves therefore confirm that the four implemented profiles produce distinct PHY behavior under the evaluated configuration.

C. End-to-End Validation

The end-to-end evaluation verifies that the composite GEO channel is applied consistently at the gNB and UE and remains compatible with complete 5G SA operation. Each trial uses paired RFsim configurations specifying the GEO composite model, elevation angle, urban environment, and forced `los` or `nlos` state. A trial is marked PASS when all three of the following conditions are satisfied:

1) The logs report the expected resolved state and effective NTN-TDL profile according to Table III.
2) The gNB and UE report consistent `GEO state` values, including elevation, slant range, FSPL correction, clutter correction, and NLOS shadow-fading terms.
3) The UE completes SIB1/SIB19 acquisition, RRC setup, NAS registration, PDU-session establishment, and user-plane interface bring-up.

The urban test matrix comprises sixteen trials: four configured GEO composite models, two forced link states, and two elevation angles (30° and 60°). Forced states make the expected effective profile deterministic. All trials met the validation criteria and completed 5G SA attachment and user-plane establishment, as summarized in Table VIII.

The effective profiles match the OAI-specific selection policy in Table III: tests 2, 4, 5, and 7 exercise remapping, while the remaining tests retain the profile associated with the configured state. The logs also show the expected elevation trend. From 30° to 60°, the relative FSPL correction decreases from 0.660 dB to 0.176 dB, while the NLOS clutter correction decreases from 3.5 dB to 0.7 dB.

VI. Conclusion and Future Work

This work integrated TR 38.811-based GEO NTN-TDL channel models into OAI RFsim. The implementation combines the NTN-TDL-A/B/C/D profiles with elevation-dependent relative FSPL and clutter corrections, reciprocal NLOS shadow fading, configurable LOS/NLOS states, and an OAI-specific initialization-time profile-selection policy. Validation checks confirmed the intended descriptors, realized power-delay structure, LOS probability, NLOS shadow-fading statistics, and elevation-dependent channel parameters. PHY-level tests demonstrated distinct BLER behavior across the four profiles, while all sixteen end-to-end trials at 30° and 60° completed the expected profile selection, 5G SA attachment, and user-plane establishment. The resulting implementation enables reproducible full-stack GEO NTN experiments in OAI with channel behavior beyond delay-only emulation. Future work will extend the GEO channel with additional TR 38.811 large-scale effects, LOS shadow fading, elevation-aware timing consistent with SIB19, dynamic LOS/NLOS profile evolution, and broader deployment scenarios. The implementation and validation artifacts are being prepared for upstream submission to the OAI `develop` branch.

Acknowledgment

This research was supported by the 6G-TWIN project under the SNS JU Horizon Europe program with Grant Agreement No. 101136314.

References

[1] 3GPP, "Study on New Radio (NR) to support non-terrestrial networks," 3rd Generation Partnership Project (3GPP), Technical Report (TR) 38.811, Oct. 2019, release 15. [Online]. Available: https://portal.3gpp.org/desktopmodules/Specifications/SpecificationDetails.aspx?specificationId=3234

[2] OpenAirInterface Software Alliance, "OpenAirInterface5G: OpenAirInterface 5G Wireless Implementation," 2015, gitLab repository, Apache License 2.0. Accessed: 2026-06-10. [Online]. Available: https://gitlab.eurecom.fr/oai/openairinterface5g

[3] MathWorks, "Model NR NTN Channel," Satellite Communications Toolbox documentation, 2024, accessed Jun. 2026. [Online]. Available: https://nl.mathworks.com/help/satcom/ug/model-nr-ntn-channel.html

[4] T. Düe, M. Vakilifard, C. Bockelmann, D. Wübben, and A. Dekorsy, "An open source channel emulator for non-terrestrial networks," in *Advanced Satellite Multimedia Systems Conference/Signal Processing for Space Communications Workshop (ASMS/SPSC 2025)*, 2025.

[5] M. Sandri, M. Pagin, M. Giordani, and M. Zorzi, "Implementation of a channel model for non-terrestrial networks in ns-3," in *Proc. Workshop on ns-3 (WNS3)*, Arlington, VA, USA, Jun. 2023, arXiv:2305.05544.

TABLE VI
GEO RESOLVER STATISTICAL AND LARGE-SCALE CHECKS

Validation item	Condition	Observed
GEO LOS-prob. error	50000 draws, 10/30/60 deg	max abs. err = 0.0021
GEO shadow-sigma err.	50000 draws, NLOS, 10/30/60 deg	max abs. err = 0.068 dB; 95% samp. half-width < 0.10 dB
GEO urban LOS delay spread	$10^\circ/30^\circ/60^\circ$	10.715 / 6.166 / 4.074 ns
GEO urban NLOS delay spread	$10^\circ/30^\circ/60^\circ$	61.660 / 17.783 / 9.772 ns
GEO relative FSPL increment	$10^\circ/30^\circ/60^\circ$	1.093 / 0.660 / 0.176 dB
GEO remap matrix	30°, urban, A/B/C/D $\times$ LOS/NLOS	matches Table III

TABLE VII
FIRST-ROUND BLER AT 2 DB SNR; VALUES ARE ORDERED AS NTN-TDL-A/B/C/D.

Unitary Simulator	BLER A/B/C/D
`nr_dlsim`	0.104 / 0.137 / 0.0278 / 0.0592
`nr_ulsim`	0.1908 / 0.2368 / 0.0296 / 0.0668

TABLE VIII
END-TO-END RFSIM VALIDATION AT 30° AND 60° ELEVATION UNDER URBAN CONDITIONS. PASS DENOTES SUCCESSFUL PROFILE SELECTION, GEO-STATE VERIFICATION, 5G SA ATTACHMENT, AND USER-PLANE ESTABLISHMENT.

Test	Configured	State	Effective	Remap	Attach 30°	Attach 60°
1	A	NLOS	A	no	PASS	PASS
2	A	LOS	C	yes	PASS	PASS
3	B	NLOS	B	no	PASS	PASS
4	B	LOS	D	yes	PASS	PASS
5	C	NLOS	A	yes	PASS	PASS
6	C	LOS	C	no	PASS	PASS
7	D	NLOS	B	yes	PASS	PASS
8	D	LOS	D	no	PASS	PASS

[6] Magister Solutions, “SNS3: Satellite network simulator 3,” 2024, ns-3 satellite extension module developed under ESA contract. Accessed: 2026-06-11. [Online]. Available: https://github.com/sns3/sns3-satellite

[7] Software Radio Systems, “srsRAN Project: Open-source O-RAN 5G RAN,” 2023, gitLab/GitHub repository. Accessed: 2026-06-11. [Online]. Available: https://github.com/srsran/srsRAN_Project

[8] ——, “srsRAN gNB for 5G NTN,” srsRAN Project documentation, 2024, accessed: 2026-06-11. [Online]. Available: https://docs.srsran.com/projects/project/en/latest/tutorials/source/ntn/source/index.html

[9] S. Kumar, A. K. Meshram, A. Astro, J. Querol, S. Chatzinotas, T. Schlichter, G. Casati, T. Heyn, F. Völk, S. Kaya, R. T. Schwarz, A. Knopp, P. Marques, L. Pereira, R. Magueta, A. Kapovits, and F. Kaltenberger, “OpenAirInterface as a platform for 5G-NTN research and experimentation,” in *Proc. IEEE Future Netw. World Forum (FNWF)*, 2022, pp. 500–506.

[10] S. Kumar, A. Astro, O. Kodheli, J. Querol, S. Chatzinotas, T. Schlichter, G. Casati, T. Heyn, F. Völk, S. Kaya, R. T. Schwarz, A. Knopp, A. Kapovits, and F. Kaltenberger, “5G-NTN GEO-based in-lab demonstrator using OpenAirInterface5G,” in *Proc. 11th Adv. Satellite Multimedia Syst. Conf. (ASMS)*, 2022.

[11] S. Kumar, O. Kodheli, A. Astro, J. Querol, S. Chatzinotas, G. Casati, T. Schlichter, T. Heyn, H. Cheporniuk, F. Völk, R. T. Schwarz, A. Knopp, A. Kapovits, and F. Kaltenberger, “5G-NTN GEO-based over-the-air demonstrator using OpenAirInterface,” in *Proc. 39th Int. Commun. Satellite Syst. Conf. (ICSSC)*, 2022.

[12] F. Völk, T. Schlichter, S. Kumar, R. T. Schwarz, A. Knopp, M. Hammouda, T. Heyn, J. Querol, S. Chatzinotas, and A. Kapovits, “5G Non-Terrestrial Networks With OpenAirInterface: An experimental study over GEO satellites,” *IEEE Access*, vol. 12, pp. 155 098–155 109, 2024.

[13] S. Kumar, C. K. Sheemar, J. Querol, T. Yilmaz, S. Chatzinotas, M. Hammouda, O. Kodheli, A. Astro, and F. Kaltenberger, “5G NTN LEO based demonstrator using OpenAirInterface5G,” in *IET Conf. Proc.*, vol. 2023, no. 48, 2023, pp. 69–75.

[14] 3GPP, “TR 38.821: Solutions for NR to support Non-Terrestrial Networks (NTN),” 3rd Generation Partnership Project (3GPP), Technical Report TR 38.821, 2021, Release 16; available from the 3GPP specification portal. [Online]. Available: https://www.3gpp.org/dynareport/38821.htm